

Supporting Information

Enhancing the Efficiency of PVDF-Based Piezoelectric Catalysis through Water-Induced Polarization and Micro-Nano Composite Strategy

Haitao Li,^{*a} Yingying Zhang,^{a,b} Han Dai,^a Veronica Pereira,^c Junfeng Zhao^{*a} and Hiang Kwee Lee^{*c, d}

^aLaboratory of Advanced Light Alloy Materials and Devices, Postdoctoral Workstation of Nanshan Group Co., Ltd., Yantai Nanshan University, Longkou 265713, China.

^bSchool of Chemistry and Chemical Engineering, Yangzhou University, Yangzhou, 225002, PR China.

^cDivision of Chemistry and Biological Chemistry, School of Chemistry, Chemical Engineering and Biotechnology, Nanyang Technological University, 21 Nanyang Link, 637371 Singapore

^dInstitute of Materials Research and Engineering, The Agency for Science, Technology and Research (A*STAR), 2 Fusionopolis Way, #08-03, Innovis 138634, Singapore

Corresponding Author

E-mail address: htli@yzu.edu.cn (Haitao Li); zhaojunfengcc@163.com (Junfeng Zhao); hiangkwee@ntu.edu.sg (Hiang Kwee Lee)

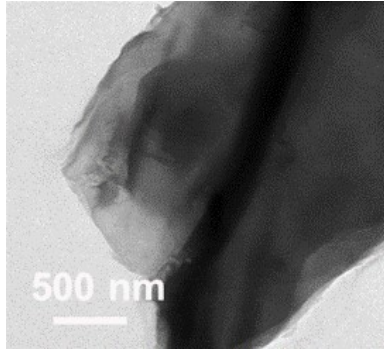


Figure S1. TEM image of rGO.

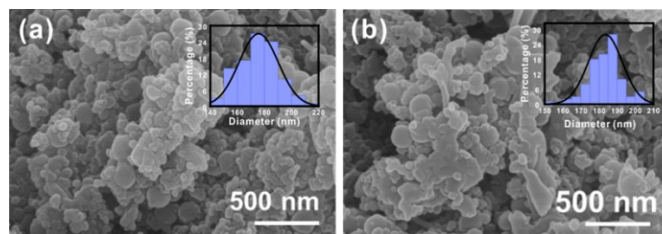


Figure S2. SEM images of (a) self-polarized PVDF (SP) and (b) self-polarized rGO/PVDF (SP/rGO).

The calculation of β phase content and related crystallinity

(1) The calculation of β phase: FTIR absorption was assumed to obey the Lambert-Beer law, the amount of the β -phase ($F(\beta)$) of PVDF was calculated using Eq (S1)¹.

$$F(\beta) = \frac{A_{\beta}}{1.26A_{\alpha} + A_{\beta}} \times 100 \% \quad (S1)$$

Here, A_{α} and A_{β} , respectively, correspond to the absorbance of the α (762 cm^{-1}) and β phases (839 cm^{-1}) of PVDF. The β phase content of original PVDF, SP and SP/rGO_{1.5} are 14%, 91%, 95%, respectively.

(2) The calculation of related crystallinity: The crystallinities of original PVDF, SP and SP/rGO_{1.5} are calculated according to their temperature increase curves using Eq. (S2)².

$$X_c = \frac{\Delta H_f}{\Delta H_f^* \cdot \phi} \times 100 \% \quad (S2)$$

Where ΔH_f is the sample enthalpy of fusion, calculated from heating DSC curve, ΔH_f^* is the heat of fusion of perfectly crystalline PVDF from literature (104.7 J g^{-1}) and ϕ is the weight fraction of PVDF in the samples. The crystallinity for original PVDF, SCP₀ and SCP_{1.5} are 23 %, 37%, 40%, respectively.

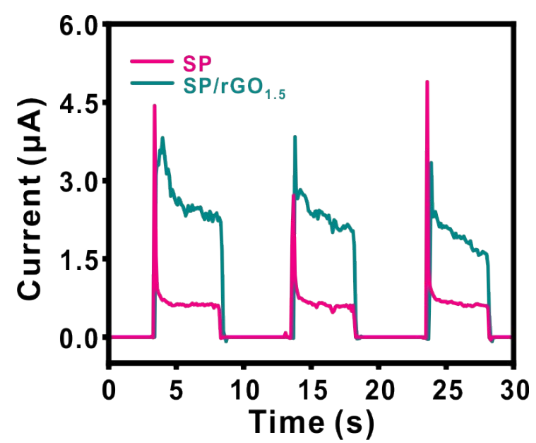


Figure S3. Piezoelectric current of (a) SP and (b) SP/rGO_{1.5}.

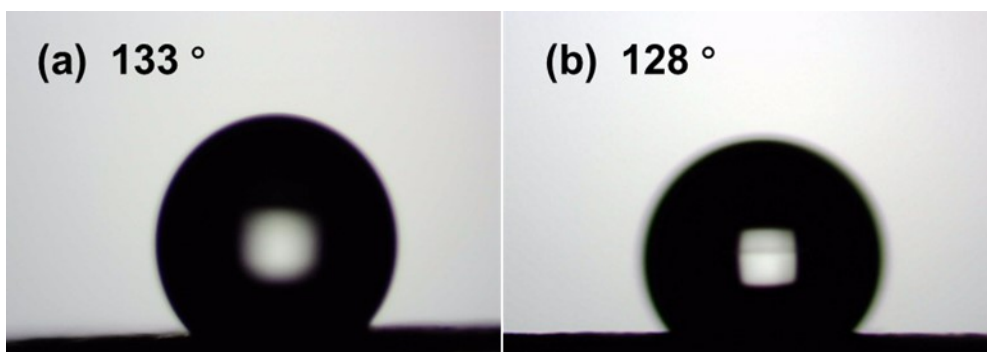


Figure S4. Contact angle images of a sessile water droplet on (a) SP and (b) SP/rGO_{1.5}.

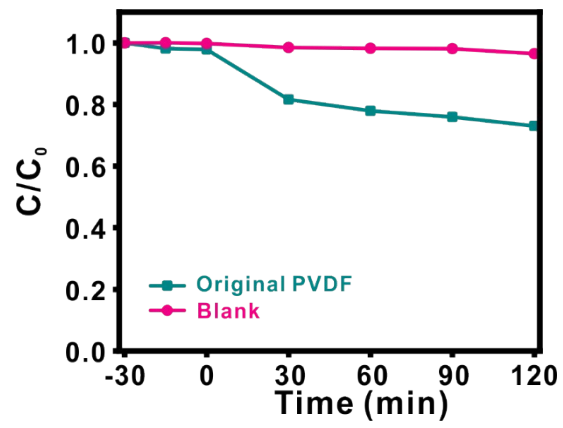


Figure S5. Piezocatalytic degradation of 15 mL RhB solution (100 mg L^{-1} , $\text{pH}=7$, $30 \text{ }^\circ\text{C}$) under 240 W ultrasonication. Comparison of normalized absorbance between 15 mg pristine PVDF and blank control.

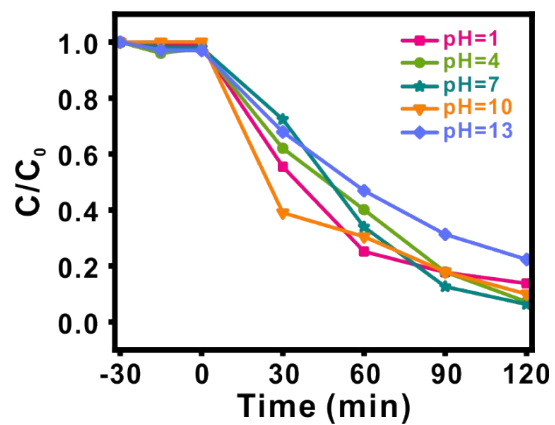


Figure S6. Time-dependent plot of normalized RhB concentration (15 mL, 100 mg L⁻¹; 30 °C) under 240 W ultrasonication at different pH environment (1 - 13) and in the presence of SP/rGO_{1.5} (15 mg).

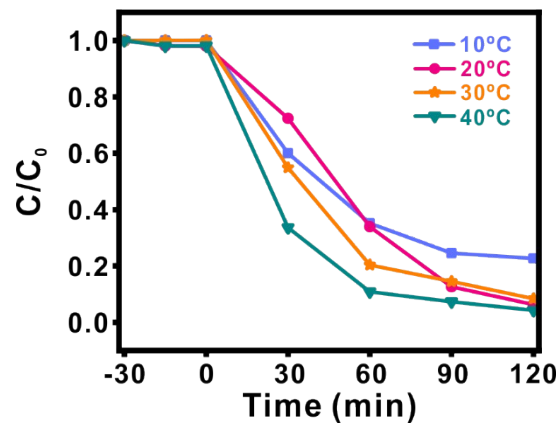


Figure S7. Time-dependent plot of normalized RhB concentration (15 mL; pH =7; 30 °C) under 240 W ultrasonication at different reaction temperature (10 - 40°C) and in presence of SP/rGO_{1.5} (15 mg).

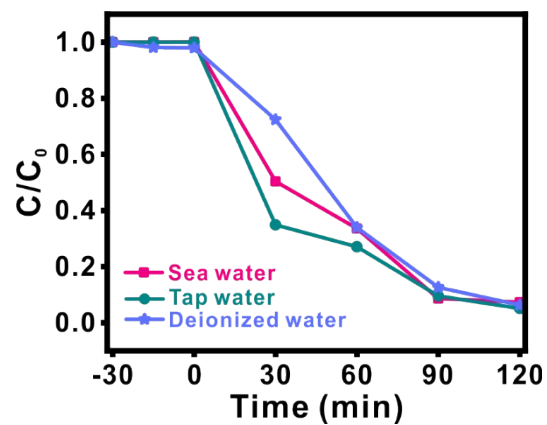


Figure S8. Time-dependent plot of normalized RhB concentration (15 mL; pH =7; 30 °C) under 240 W ultrasonication when using different water samples (DI water, tap water and sea water) and in the presence of SP/rGO_{1.5} (15 mg).

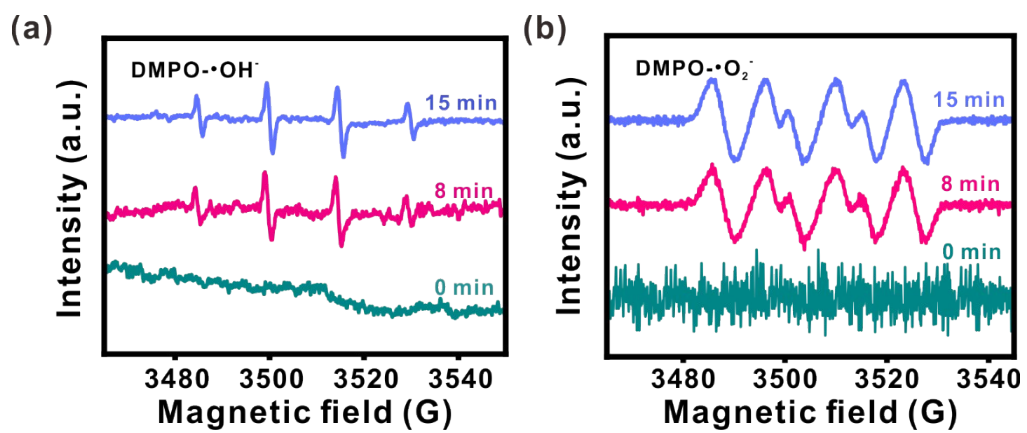


Figure S9. (a) DMPO-·OH and (b) DMPO-·O₂⁻ obtained from SP/rGO_{1.5} with different ultrasonication time.

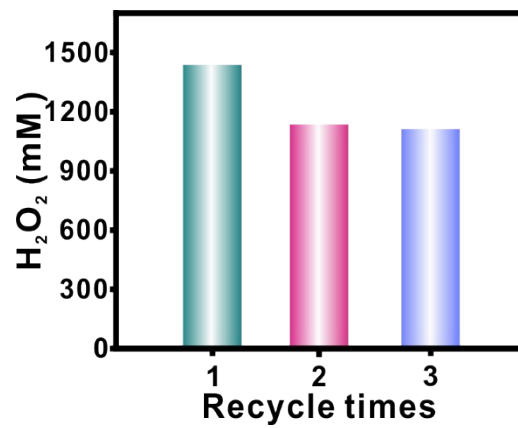


Figure S10. Comparison of H₂O₂ production rate by SP/rGO_{1.5} over three successive cycles.

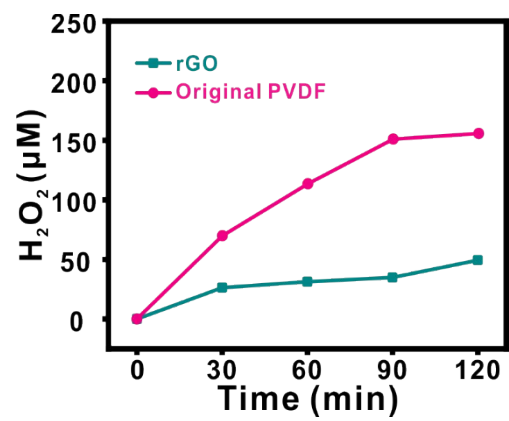


Figure S11. Time-dependent piezocatalytic H₂O₂ productions by rGO and pristine PVDF under 300 W ultrasonication.

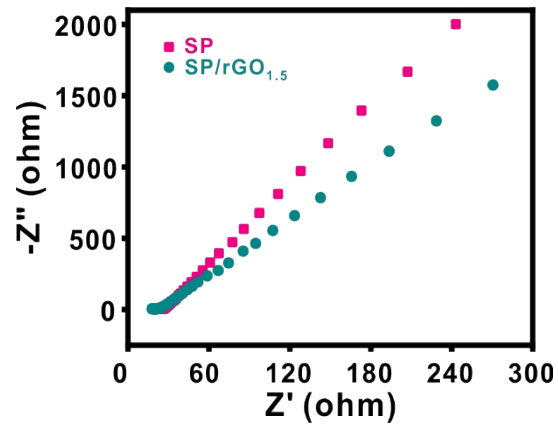


Figure S12. Electrochemical impedance spectroscopy characterization of SP and SP/rGO_{1.5}.

Table S1. Comparison of the organic degradation and H₂O₂ production by SP/rGO_{1.5} with other previously reported piezoelectric catalysts.

| Material of catalyst, Synthesis method | Content of catalyst | Reaction solution | Frequency and power of ultrasound | Time, min | Degradation ratio, % | Generating rate of H ₂ O ₂ , mmol g _{cat} ⁻¹ h ⁻¹ |
|---|---------------------|---|-----------------------------------|-----------|----------------------|--|
| Nano kaolinite-MWCNT/PVDF film ³ one-step solution casting method | 1x1cm | 15 mL, 2.5 ppm RhB | 33 kHz, 50 W | 45 | ~96, 99 | |
| Ag@LiNbO ₃ /PVDF ⁴ The solvent casting method | d=2.5 cm | 10 mL, 10 mg/L MB | 40 kHz, 70 W | 180 | ~89 | |
| αFe ₂ O ₃ /PVDF ⁵ electrospinning | 7 mg | 20 mL, 10 mg/L MB | 18 kHz, 250 W | 60 | ~60.4 | |
| BNT/PVDF ⁶ , a “sol-gel-electrospinning” method | 100 mg | 100 mL, 50 mg/L RhB | 45 kHz, 200 W | 180 | ~76.6 | |
| BNBT-x ⁷ , one-step solvothermal method. | 100 mg | 50 mL, 10 mg/L RhB | 18 kHz, 250 W | 60 | ~73 | |
| PCN/PVDF-HFP ⁸ | 50 mg | 8 mL H ₂ O containing 2mL EtOH | 40 kHz, 300 W | 120 | | 0.668 |
| SiO ₂ /PVDF-HFP ⁹ | 50 mg | 8 mL H ₂ O containing 2mL EtOH | 40 kHz, 300 W | 60 | | 0.492 |
| CNT/PVDF ¹⁰ phase separation by nanosization | 15 mg | 15 mL, 40 mg L ⁻¹ RhB | 40 kHz, 240 W | 120 | ~98 | |
| | 25 mg | 8 mL H ₂ O containing 2mL EtOH | 40 kHz, 300 W | 120 | | 13.51 |
| rGO/PVDF phase separation by nanosization | 15 mg | 15 mL, 100 mg L ⁻¹ RhB | 40 kHz, 240 W | 120 | ~93.7 | |
| | 5 mg | 8 mL H ₂ O containing 2mL EtOH | 40 kHz, 300 W | 120 | | 95.8 |

Note and references

1. S. Huang, S. Hong, Y. Su, Y. Jiang, S. Fukushima, T. M. Gill, N. E. D. Yilmaz, S. Tiwari, K.-i. Nomura, R. K. Kalia and Flame, *Combust Flame*, 2020, **219**, 467-477.
2. C. Merlini, G. Barra, T. M. Araujo and A. Pegoretti, *RSC Adv*, 2014, **4**, 15749-15758.
3. D. Mondal, S. Bardhan, N. Das, J. Roy, S. Ghosh, A. Maity, S. Roy, R. Basu and S. Das, *Nano Energy*, 2022, **104**.
4. G. Singh, M. Sharma and R. Vaish, *ACS Appl Mater Interfaces*, 2021, **13**, 22914-22925.
5. F. Orudzhev, S. Ramazanov, D. Sobola, P. Kaspar, T. Trčka, K. Částková, J. Kasty, I. Zvereva, C. Wang, D. Selimov, R. Gulakhmedov, M. Abdurakhmanov, A. Shuaibov and M. Kadiev, *Nano Energy*, 2021, **90**.
6. X. Zhou, Q. Sun, Z. Xiao, H. Luo and D. Zhang, *J. Environ*, 2022, **10**.
7. L. Jiang, N. Xie, Y. Hou, H. Fu, J. Zhang, H. Gao and Y. Liao, *Catal Commun*, 2023, **181**, 106735.
8. Z. Chen, J. Zhuang, C. Liu, M. Chai, S. Zhang, K. Teng, T. Cao, Y. Zhang, Y. Hu, L. Zhao and Q. An, *ChemElectroChem*, 2022, **9**.
9. L. Wang, Z. Chen, Y. Zhang, C. Liu, J. Yuan, Y. Liu, W. Ge, S. Lin, Q. An and Z. Feng, *Chem Asian J*, 2022, **17**, e202200278.
10. Y. Zhang, C. Chong, W. Tong, H. Li, H. K. Lee and J. Han, *Colloids and Surfaces A: Physicochemical and Engineering Aspects*, 2023, **677**.